Lithium Batteries Hot Paper

Deutsche Ausgabe: DOI: 10.1002/ange.201501214
Internationale Ausgabe: DOI: 10.1002/anie.201501214

The First Introduction of Graphene to Rechargeable Li–CO_2 Batteries**

*Zhang Zhang, Qiang Zhang, Yanan Chen, Jie Bao, Xianlong Zhou, Zhaojun Xie, Jinping Wei, and Zhen Zhou**

Abstract: *The utilization of the greenhouse gas CO_2 in energy-storage systems is highly desirable. It is now shown that the introduction of graphene as a cathode material significantly improves the performance of Li–CO_2 batteries. Such batteries display a superior discharge capacity and enhanced cycle stability. Therefore, graphene can act as an efficient cathode in Li–CO_2 batteries, and it provides a novel approach for simultaneously capturing CO_2 and storing energy.*

Rechargeable Li–O_2 batteries have been attracting much attention owing to their high specific energy density, which is comparable to that of gasoline.[1,2] However, the development of batteries that operate in air still represents a great challenge owing to the influence of moisture and CO_2 on their performance.[1,3] Recently, Zhou and Zhang developed Li–air batteries that operate in ambient air, and they found that reversible reactions related to Li_2CO_3, which is the product of Li_2O_2 with CO_2 in air, occurred.[4] Although CO_2 contamination was found to increase the discharge capacity of the cell, the presence of CO_2 during discharge dramatically influenced the electrochemical process.[3] This phenomenon was also reported by Takechi et al.; when batteries were operated with a mixture of O_2 and CO_2, the capacity could reach three times that of the batteries operated with pure O_2.[5] Reversible Li–CO_2/O_2 (1:1, v/v) batteries were also investigated with different dielectric electrolytes, and it was found that dimethyl sulfoxide (DMSO) might be the optimal electrolyte for the reversible formation and decomposition of Li_2CO_3.[6] However, in the above cases, CO_2 was not involved in the electrochemical reactions that proceed with electron transfer. Recently, it was reported that a true Li–CO_2 battery (without O_2) could be cycled and exhibited a moderate discharge capacity.[7] The theoretical voltage of approximately 2.8 V can be determined according to the following equation: $4\,Li + 3\,CO_2 \rightarrow 2\,Li_2CO_3 + C$.[7,8] Li–$CO_2$ batteries were also developed by Archer et al., but their primary Li–CO_2 batteries only showed good discharge capacities at high temperatures.[8]

CO_2 is now recognized as a leading greenhouse gas, and its rising emission has been implicated in global climate changes.[9] Its recycling and utilization in energy systems is thus globally investigated. In our previous work, it was confirmed that CO_2 (CO_3^{2-}) could be reduced to low-valent carbon at room temperature by making use of the excellent catalytic activities of transition-metal nanoparticles.[10] Based on this electrochemical catalytic conversion mechanism, the corresponding nanomaterials were also explored for many other applications.[11–15] Furthermore, Azuma et al. also investigated the electrochemical reduction of CO_2 (CO_3^{2-}) on 32 metal electrodes in $KHCO_3$ solutions.[16] We believe that with Li–CO_2 batteries, tremendous progress could be made in terms of CO_2 recycling while achieving an excellent electrochemical performance.

Herein, we describe the first introduction of graphene into Li–CO_2 batteries. Graphene has also attracted much attention as an ideal cathode material for Li–O_2 batteries owing to its excellent electrical conductivity, large surface area, and high electrochemical stability. It also provides efficient diffusion channels for O_2, enough space for product storage, and active sites for electrochemical reactions.[17–20] We believed that graphene could also play an important role in Li–CO_2 batteries, significantly promoting electrochemical processes and enhancing the cycle stability of rechargeable Li–CO_2 batteries.

Scanning electron microscopy (SEM) and transmission electron microscopy (TEM) images of graphene are presented in Figure 1 a, b; they show the typical interconnected thin graphene nanosheets with a porous, wrinkled structure. These unique structures provide an ideal porosity that is suitable for electrolyte wetting and CO_2 diffusion, thus improving the electrochemical activity of Li–CO_2 batteries.

The electrochemical performance of graphene was first evaluated by using it as the cathode in Li–CO_2 batteries. The

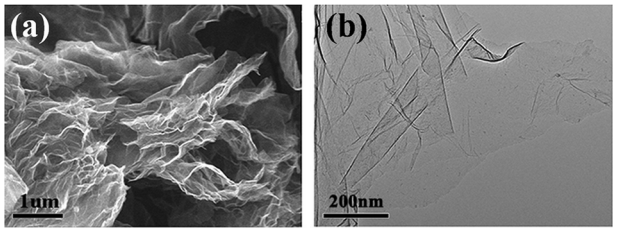

Figure 1. a) SEM and b) TEM images of graphene.

[*] Z. Zhang, Q. Zhang, Y. N. Chen, J. Bao, X. Zhou, Z. J. Xie, J. P. Wei, Prof. Z. Zhou
Tianjin Key Laboratory of Metal and Molecule Based Material Chemistry, Key Laboratory of Advanced Energy Materials Chemistry (Ministry of Education), Institute of New Energy Material Chemistry, Collaborative Innovation Center of Chemical Science and Engineering (Tianjin), Nankai University
Tianjin 300071 (P.R. China)
E-mail: zhouzhen@nankai.edu.cn

[**] This work was supported by the NSFC (21473094 and 21421001) and the MOE Innovation Team (IRT13022) in China. We thank Dr. L. W. Su (ZJUT) for his initial efforts in this project and Prof. H. Li (IOP, CAS) for constructive discussions.

Supporting information for this article is available on the WWW under http://dx.doi.org/10.1002/anie.201501214.

first discharge–charge measurements were performed in a voltage range of 2.2–4.3 V. Both the applied current density (in $mA\,g^{-1}$) and the achieved specific capacity (in $mAh\,g^{-1}$) were normalized to the weight of the graphene nanosheets. The solvent tetraethylene glycol dimethyl ether (TEGDME) is comparatively stable up to 4.4 V,[7,21] and it can thus be applied to Li–CO_2 batteries. First, we utilized cyclic voltammetry (CV) to explore the catalytic activity of graphene in Li–CO_2 batteries from 4.5 to 2 V (Figure 2a). Graphene exhibited evident cathodic and anodic peaks under CO_2 atmosphere, and CO_2 was indeed involved in the electrochemical

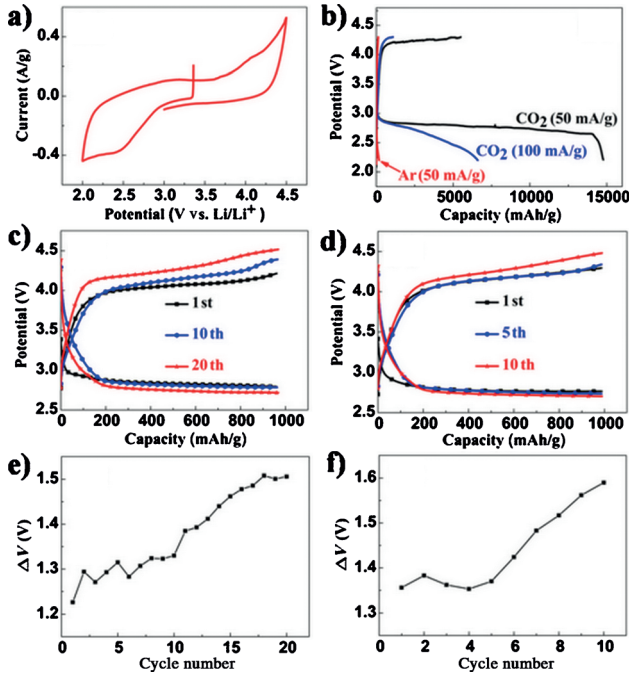

Figure 2. a) CV curves of batteries with graphene cathodes working in CO_2 at a scan rate of $0.2\ mV\,s^{-1}$. b) The initial discharge curves of the batteries with graphene cathodes at a current density of $50\ mA\,g^{-1}$ and $100\ mA\,g^{-1}$ in CO_2 atmosphere, as well as at $50\ mA\,g^{-1}$ in Ar atmosphere. c, d) Curtailing capacity of $1000\ mAh\,g^{-1}$ at a current density of $50\ mA\,g^{-1}$ (c) or $100\ mA\,g^{-1}$ (d). e, f) Voltage hysteresis between the charge–discharge curves at a current density of $50\ mA\,g^{-1}$ (e) or $100\ mA\,g^{-1}$ (f).

reaction. The discharge–charge curves of Li–CO_2 batteries with the graphene cathode at a current density of $50\ mA\,g^{-1}$ and $100\ mA\,g^{-1}$ are shown in Figure 2b, and the graphene cathode delivered capacities of $14722\ mA\,g^{-1}$ and $6600\ mA\,g^{-1}$, respectively. Furthermore, the graphene cathode exhibited a stable discharge platform of approximately 2.77 V at a current density of $50\ mA\,g^{-1}$, which is extremely close to the theoretical equilibrium voltage of Li–CO_2 batteries.[8] This was the first time that graphene was introduced into Li–CO_2 batteries to yield systems with an excellent discharge capacity. Although the charge process shows a higher voltage and lower columbic efficiency than graphene-based Li–O_2 batteries even at a low current density,[18,22] our results made us confident that the electrochemical performance of Li–CO_2 batteries could indeed be greatly improved compared with those based on Ketjen black (KB; see the Supporting Information, Figure S1 and Table S1). For comparison, the discharge–charge performance was also tested with argon as the working gas, and the system was found to exhibit a small discharge capacity (Figure 2b and Figure S2). For the cycling tests, the cells were discharged and charged with a cut-off capacity of $1000\ mAh\,g^{-1}$ at a current density of $50\ mA\,g^{-1}$ or $100\ mA\,g^{-1}$. The cells showed good performance over 20 cycles with stable discharge–charge voltage platforms at a current density of $50\ mA\,g^{-1}$ (Figure 2c). The batteries also performed well over ten cycles with stable discharge–charge voltage platforms at a current density of $100\ mA\,g^{-1}$ (Figure 2d). Furthermore, it is apparent that the overpotential increases as the cycle proceeds, which is attributed to the accumulation of inactive Li_2CO_3.[7] Garcia Lastra et al. pointed out that the charge transport in Li_2CO_3 was even poorer than that in Li_2O_2,[23] and CO_2 evolution from Li_2CO_3 during the charging process was found to occur only at very high potentials compared with O_2 evolution from Li_2O_2.[3] In previous reports, Li–CO_2 batteries could only operate at high temperatures[8] or at a low current density ($30\ mA\,g^{-1}$),[7] and always displayed unsatisfactory electrochemical performances.

However, we were able to utilize graphene as the cathode at a higher current density of $50\ mA\,g^{-1}$, and the batteries could be operated reversibly for 20 cycles at a voltage of up to 4.5 V with stable discharge (>2.75 V) and charge (<4.3 V) platforms. Even at a much higher current density ($100\ mA\,g^{-1}$), the graphene cathode (Figure 2b,c) also exhibited a lower overpotential and better cyclability than KB (Figure S1). Although Li–CO_2 batteries with graphene cathodes could be operated for over 20 cycles, their overpotential obviously increased (Figure 2b,c), indicating that the instability of the battery system leaves room for further improvement.

To investigate the details of the discharge/charge processes in Li–CO_2 batteries, the graphene cathodes were analyzed by SEM during the first discharge/charge cycles. The characterization of the discharge/charge processes was limited to a cut-off capacity of $1000\ mAh\,g^{-1}$ at a current density of $50\ mA\,g^{-1}$. After the first discharge, the products were deposited on porous graphene and accumulated on the graphene cathode; it is noteworthy that the graphene was fully covered with the discharge products (Figure 3a). After the subsequent charging process, the graphene nanosheets recovered their porous structure with large spaces between them (Figure 3b). To accurately characterize the discharge products of the first cycle, they were analyzed by Fourier transform infrared (FTIR) spectroscopy. As shown in Figure 3c, the characteristic peaks of Li_2CO_3 were observed at $1427\ cm^{-1}$ and $862\ cm^{-1}$, which are consistent with the standard patterns of Li_2CO_3 (Figure S3a) and previous reports.[7,24] Other peaks might be due to the cleaning solution lithium bis(trifluoromethanesulfonyl)imide (LiTFSI)/TEGDME (Figure S3b), which could also be clearly observed in the FTIR spectrum of the charged cathode. After the charge process, the peaks of Li_2CO_3 decreased in intensity and finally disappeared, and graphene indeed exhibited an

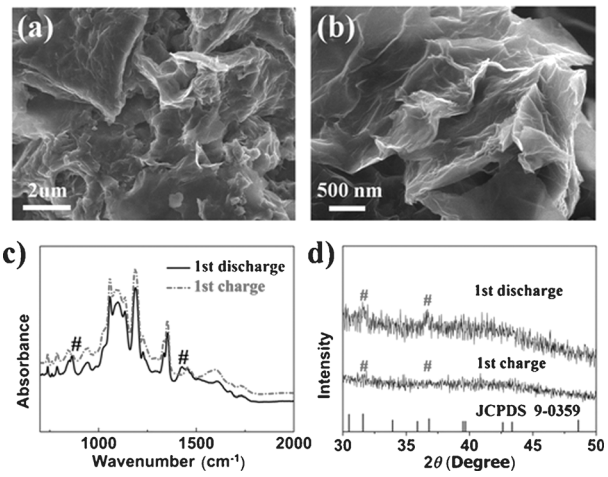

Figure 3. a, b) SEM images of graphene cathodes after the first discharge (a) and after the first charge (b). c) FTIR spectra and d) XRD patterns of the graphene cathode after the first discharge and charge processes. # indicates peaks corresponding to Li_2CO_3.

excellent catalytic activity in the decomposition of Li_2CO_3. The discharge/charge products were also analyzed by X-ray diffraction (XRD) of the cathode (Figure 3 d). The Li_2CO_3 material that could be observed during the first discharge process corresponds to standard Li_2CO_3 (JCPDS 9-0359). After the subsequent charge process, the peaks of Li_2CO_3 had obviously disappeared. Furthermore, the XRD curve became flat and smooth after the charge process, indicating the decomposition of the discharge products. These results confirmed the excellent electrochemical activity of graphene in Li–CO_2 batteries.

This is the first time that graphene has ben introduced into Li–CO_2 batteries to yield systems with improved performances, even though graphene has previously been applied to Li–O_2 batteries.[17,18,20,25] Graphene indeed exhibited an excellent electrochemical activity in Li–CO_2 batteries. Compared with Li–O_2 batteries that contained individual KB,[26,27] the graphene-based batteries indeed showed a higher electrochemical performance. We also confirmed that addition of graphene to Li–CO_2 batteries led to a higher capacity, a lower overpotential, and better cyclability than KB owing to their different structures (Figure S4).

To confirm the presence of carbon, a platinum net was used as the cathode in Li–CO_2 batteries. These batteries were discharged to 2.2 V and then subjected to ultrasound for electron energy loss spectroscopy (EELS; Figure S5), which gave a typical spectrum with visible edges at 282 eV, corresponding to the characteristic K shell ionization energy of carbon.[28,29] The two bands corresponding to carbon can be well assigned to transitions from the 1s orbital to the π^* antibonding orbital, followed by another band attributed to 1s–σ^* transitions. It is not clear whether the reaction mechanism is the same for Li–CO_2 batteries with a platinum net or graphene as the cathode. Thus, the introduction of a platinum net was only used to confirm the presence of carbon as a reference.

In addition, we also performed first-principles computations to identify the discharge product. The possible reactions with their open-circuit voltages are listed in Table S2. It can be seen that the calculated voltage of the reaction $4Li + 3CO_2 = C + 2Li_2CO_3$ is 2.66 V, which is roughly consistent with the experimental data (2.8 V). Other reactions can be excluded.

To illustrate the excellent catalytic activity of the graphene cathodes, the electrochemical performance of the Li–CO_2 battery with a graphene cathode was compared with those of batteries with other cathodes (Table S1). These reference data summarize recent progress in the development of Li–CO_2 batteries. Although graphene cathodes have exhibited excellent electrochemical activity in Li–CO_2 batteries, including higher capacities, longer cyclabilities, and lower overpotentials, their kinetic parameters still have to be greatly improved to reach the efficiencies of Li–O_2 batteries with graphene-based cathodes.[19,30]

In conclusion, we have reported the first introduction of graphene into Li–CO_2 batteries. The Li–CO_2 batteries with graphene cathodes delivered a high discharge capacity of up to 14774 mAh g^{-1} and a stable cyclability over 20 cycles at a current density of 50 mA g^{-1}. Although the current Li–CO_2 batteries were operated at a low current density with a high overpotential, we believe that cathode materials with excellent electrical conductivity, a porous structure, and catalytic activity can be useful for utilizing and capturing CO_2, enabling the development of commercially viable, rechargeable energy-storage devices.

Experimental Section

Material preparation: Few-layered graphene was prepared from natural flake graphite powder through a modified Hummers' method followed by a thermal reduction.[10]

Material characterization**:** XRD was performed on a D/MAX III diffractometer with $Cu_{K\alpha}$ radiation. Field emission SEM (FESEM) images were obtained on a JEOL-JSM7500 microscope. TEM images were taken on a FEITecnai G2F-20 equipped with EELS. FTIR spectroscopy was conducted on a NicoletMAGNA-560 FTIR spectrometer using KBr pellets.

Electrochemical tests: The electrochemical performances were measured in Swagelok cells with a 1.0 cm^2 hole in the cathode, which enabled CO_2 to flow in. The cells were assembled in a glove box filled with high-purity argon (O_2 and H_2O content <1 ppm). For the cathode preparation, a slurry was obtained by mixing graphene and polyvinylidenefluoride (PVDF) in a mass ratio of 9:1. The slurry was uniformly deposited on a circular piece of carbon paper (1.12 cm^2 with 0.3–0.5 mg of active material), and then dried in an oven at 80 °C. Li foil was used as the anode and a polytetrafluoroethylene (PTFE) membrane as the separator. LiTFSI (1 mol L^{-1}) dissolved in TEGDME was used as the electrolyte. Discharge/charge tests were conducted on a LAND-CT2001A tester, and the cells were discharged to 2.2 V and then recharged to 4.3 V. Cyclic voltammograms were recorded with a Zahner–Elektrik IM6e electrochemical workstation within 2–4.5 V. Cycling tests were conduced with a cut-off capacity of 1000 mAh g^{-1} at a current density of 50 mA g^{-1} and 100 mA g^{-1} (i.e., the cells were discharged and charged for 20 h and 10 h, respectively).

DFT computations: First-principles computations were performed within the Vienna Ab initio Simulation Package (VASP). Density functional theory (DFT) with periodic boundary conditions was introduced to both geometry optimization and static computa-

tion. The generalized gradient approximation (GGA) to the exchange-correlation functional of PW91[31] with spin polarization was applied to our simulation. The projector augmented wave (PAW)[32] was used to describe the inner electrons of all atoms. To identify the cathode reaction, $4Li + 3CO_2 \rightarrow C + 2Li_2CO_3$, we discussed other possible reactions. The voltages for the electrochemical reactions are defined as $U = \Delta E/zF$, where z is the number of electrons transferred, and F is the Faraday constant. ΔE was evaluated according to changes in enthalpy at 0 K.

Keywords: cathode materials · electrocatalysis · graphene · lithium–air batteries

How to cite: *Angew. Chem. Int. Ed.* **2015**, *54*, 6550–6553
Angew. Chem. **2015**, *127*, 6650–6653

[1] P. G. Bruce, S. A. Freunberger, L. J. Hardwick, J. M. Tarascon, *Nat. Mater.* **2012**, *11*, 19–29.
[2] G. Girishkumar, B. McCloskey, A. C. Luntz, S. Swanson, W. Wilcke, *J. Phys. Chem. Lett.* **2010**, *1*, 2193–2203.
[3] S. R. Gowda, A. Brunet, G. M. Wallraff, B. D. McCloskey, *J. Phys. Chem. Lett.* **2013**, *4*, 276–279.
[4] T. Zhang, H. Zhou, *Nat. Commun.* **2013**, *4*, 1817.
[5] K. Takechi, T. Shiga, T. Asaoka, *Chem. Commun.* **2011**, *47*, 3463–3465.
[6] H. K. Lim, H. D. Lim, K. Y. Park, D. H. Seo, H. Gwon, J. Hong, W. A. Goddard, H. Kim, K. Kang, *J. Am. Chem. Soc.* **2013**, *135*, 9733–9742.
[7] Y. Liu, R. Wang, Y. Lyu, H. Li, L. Chen, *Energy Environ. Sci.* **2014**, *7*, 677–681.
[8] S. Xu, S. K. Das, L. A. Archer, *RSC Adv.* **2013**, *3*, 6656–6660.
[9] D. P. Schrag, *Science* **2007**, *315*, 812–813.
[10] L. Su, Z. Zhou, X. Qin, Q. Tang, D. Wu, P. Shen, *Nano Energy* **2013**, *2*, 276–282.
[11] L. Su, Z. Zhou, P. Shen, *J. Phys. Chem. C* **2012**, *116*, 23974–23980.
[12] M. Yang, Y. Zhong, L. Su, J. Wei, Z. Zhou, *Chem. Eur. J.* **2014**, *20*, 5046–5053.
[13] Y. Zhong, M. Yang, X. Zhou, Y. Luo, J. Wei, Z. Zhou, *Adv. Mater.* **2015**, *27*, 806–812.
[14] Z. Zhang, L. Su, M. Yang, M. Hu, J. Bao, J. Wei, Z. Zhou, *Chem. Commun.* **2014**, *50*, 776–778.
[15] Z. Zhang, J. Bao, C. He, Y. Chen, J. Wei, Z. Zhou, *Adv. Funct. Mater.* **2014**, *24*, 6826–6833.
[16] K. H. M. Azuma, M. Hiramoto, *J. Electrochem. Soc.* **1990**, *137*, 1772–1778.
[17] Y. Li, J. Wang, X. Li, D. Geng, R. Li, X. Sun, *Chem. Commun.* **2011**, *47*, 9438–9440.
[18] Y. Li, J. Wang, X. Li, D. Geng, M. N. Banis, R. Li, X. Sun, *Electrochem. Commun.* **2012**, *18*, 12–15.
[19] E. Yoo, H. Zhou, *ACS Nano* **2011**, *5*, 3020–3026.
[20] J. Xiao, D. Mei, X. Li, W. Xu, D. Wang, G. L. Graff, W. D. Bennett, Z. Nie, L. V. Saraf, I. A. Aksay, J. Liu, J. G. Zhang, *Nano Lett.* **2011**, *11*, 5071–5078.
[21] H. G. Jung, J. Hassoun, J. B. Park, Y. K. Sun, B. Scrosati, *Nat. Chem.* **2012**, *4*, 579–585.
[22] S. Y. Kim, H. T. Lee, K. B. Kim, *Phys. Chem. Chem. Phys.* **2013**, *15*, 20262–20271.
[23] J. M. Garcia-Lastra, J. S. G. Myrdal, R. Christensen, K. S. Thygesen, T. Vegge, *J. Phys. Chem. C* **2013**, *117*, 5568–5577.
[24] S. A. Freunberger, Y. Chen, N. E. Drewett, L. J. Hardwick, F. Barde, P. G. Bruce, *Angew. Chem. Int. Ed.* **2011**, *50*, 8609–8613; *Angew. Chem.* **2011**, *123*, 8768–8772.
[25] E. Yoo, J. Nakamura, H. Zhou, *Energy Environ. Sci.* **2012**, *5*, 6928–6932.
[26] J. J. Xu, D. Xu, Z. L. Wang, H. G. Wang, L. L. Zhang, X. B. Zhang, *Angew. Chem. Int. Ed.* **2013**, *52*, 3887–3890; *Angew. Chem.* **2013**, *125*, 3979–3982.
[27] C. K. Park, S. B. Park, S. Y. Lee, H. Lee, H. Jang, W. I. Cho, *Bull. Korean Chem. Soc.* **2010**, *31*, 3221–3224.
[28] O. Stephan, P. M. Ajayan, C. Colliex, P. Redlich, J. M. Lambert, P. Bernier, P. Lefin, *Science* **1994**, *266*, 1683–1685.
[29] L. Ci, L. Song, C. Jin, D. Jariwala, D. Wu, Y. Li, A. Srivastava, Z. F. Wang, K. Storr, L. Balicas, F. Liu, P. M. Ajayan, *Nat. Mater.* **2010**, *9*, 430–435.
[30] G. Wu, N. H. Mack, W. Gao, S. Ma, R. Zhong, J. Han, J. K. Baldwin, P. Zelenay, *ACS Nano* **2012**, *6*, 9764–9776.
[31] J. P. Perdew, J. Chevary, S. Vosko, K. A. Jackson, M. R. Pederson, D. Singh, C. Fiolhais, *Phys. Rev. B* **1992**, *46*, 6671–6687.
[32] P. E. Blöchl, *Phys. Rev. B* **1994**, *50*, 17953–17979.

Received: February 9, 2015
Revised: March 6, 2015
Published online: May 12, 2015

